Dark zone in the centre of the Arago-Poisson diffraction spot of a helical laser beam

2013 EPL 101 54005

(http://iopscience.iop.org/0295-5075/101/5/54005)

A LETTERS JOURNAL EXPLORING THE FRONTIERS OF PHYSICS

March 2013

EPL, **101** (2013) 54005 www.epljournal.org
doi: 10.1209/0295-5075/101/54005

Dark zone in the centre of the Arago-Poisson diffraction spot of a helical laser beam

O. EMILE[1], A. VOISIN[1], R. NIEMIEC[1,2], B. VIARIS DE LESEGNO[3], L. PRUVOST[3], G. ROPARS[1], J. EMILE[4] and C. BROUSSEAU[2]

[1] *URU 435 LPL, Université Rennes 1 - 35042 Rennes Cedex, France, EU*
[2] *UMR CNRS 6164 IETR, Université Rennes 1 - 35042 Rennes Cedex, France, EU*
[3] *UPR CNRS 3321 LAC, B 505, Campus d'Orsay - 91405 Orsay Cedex, France, EU*
[4] *UMR CNRS 6251 IPR, Université Rennes 1 - 35042 Rennes Cedex, France, EU*

received 29 November 2012; accepted in final form 19 February 2013
published online 19 March 2013

PACS 42.25.Fx – Diffraction and scattering
PACS 42.50.Tx – Optical angular momentum and its quantum aspects
PACS 42.87.Bg – Phase shifting interferometry

Abstract – We report on the diffraction of non-zero Laguerre Gaussian laser beams by an opaque disk. We observe a tiny circular dark zone at the centre of the usual Arago-Poisson diffraction bright spot. For such non-diffracting dark hollow beams, we have measured diameters as small as 20 μm on distances of the order of ten metres, without focalization. Diameters depend on the diffracting object size and on the topological charge of the input Laguerre Gaussian beam. These results are in good agreement with theoretical considerations. Potential applications are then discussed.

Introduction. – The Arago-Poisson spot is often mentioned in textbooks as a spectacular demonstration of the wave nature of light [1–3]. It consists of a bright spot appearing in the shadow of an uniformly illuminated opaque disk or sphere. The experiment was first proposed in 1818 by the corpuscularist Poisson to Fresnel, in an attempt to discredit Fresnel's wave theory of light [4,5]. However, Arago rapidly verified experimentally the existence of this spot, thus validating Fresnel's theory. Since, such spots have also been observed with X-rays [6], in acoustics [7] and even with molecular matter waves [8]. In optics, besides its non-diffracting properties, it has been responsible for damages in unstable cavities [9], it has been used for alignment purposes [10] in laser fusion experiments, and it has been shown to propagate in a supraluminic way [11,12].

On the other hand, new types of electromagnetic waves which carry orbital angular momentum have been reported [13,14]. These waves are also called twisted waves or helical waves since their phase fronts vary with rotation around their axis. Such unusual waves exist in optics [15], in the microwave domain [16], in acoustics [17] and for electron beams [18]. They can diffract and interfere as well [19]. Recently, it has been shown that the diffraction of this kind of waves by a disk, leads to a tiny dark spot in the middle of a bright spot that appears at the centre of the disk shadow [20]. Then this spot may break in several spots due to misalignment. One may thus wonder whether the single Arago-Poisson dark spot has also non-diffracting properties and what is the ultimate size of this kind of beams. The aim of this letter is to explore these dark-hollow-diffracted-beam characteristics (size, propagation, symmetry) and to investigate for potential applications.

Experimental set-up. – The laser source is a 1 mW He-Ne laser (Uniphase DIN 58126, waist $w = 625$ μm) operating at $\lambda = 633$ nm (see fig. 1). The fundamental Gaussian beam from the laser is transformed to a Laguerre Gaussian (LG) beam with an order l varying from $l = 1$ to 8 using a vortex phase plate (RPC Photonics), also called spiral phase plate, adapted for the wavelength. A spiral phase plate is one of the tools to generate LG beams [15,21]. It has also been used as a coronograph [22]. The order l of the beam (also called the topological charge) is the phase variation times 2π around the axis of the beam during one turn. This vortex plate has a thickness that varies when rotating around the plate axis (see inset of fig. 1). It thus twists the plane phase of the initial laser beam around its axis. Such a beam carries an orbital angular momentum that equals $l\hbar$ per photon [13].

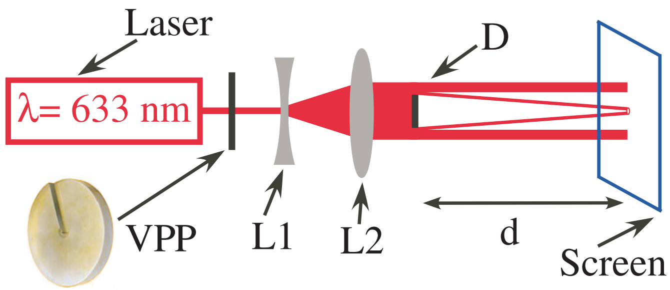

Fig. 1: (Colour on-line) Experimental set-up. VPP: vortex phase plate; L1, L2: lenses; D: diffracting disk; d: distance between the diffracting disk and the screen. Inset: schematic drawing of the VPP showing the thickness variation of the plate that induces the phase variation of the helical beam.

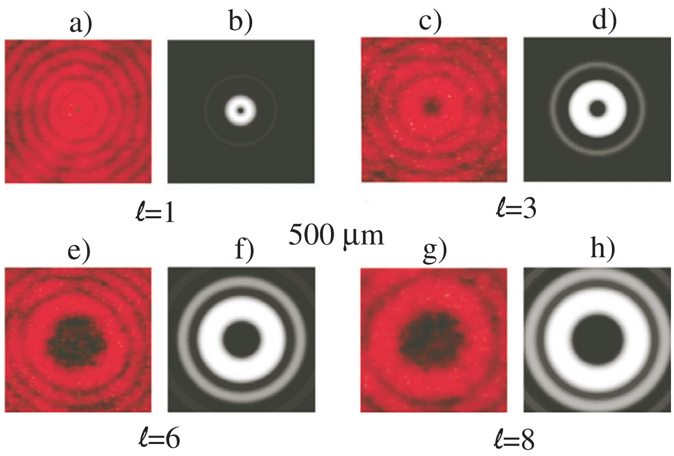

Fig. 2: (Colour on-line) Pictures of the diffracted beam at a distance of $d=3.5$ m. a), c), e), g): experimental data; b), d), f), h): corresponding calculations.

So that the laser beam size matches the size of the phase plate, the plate is then located 1 m after the end of the laser. The laser beam is expanded using two lenses that actually accounts for a telescope, in order to correspond to the size of the diffracting object. We choose a diffracting object that has the same cylindrical symmetry as the laser beam. We use 7, 12, and 14 mm diameter diffracting opaque disks which are exactly centred with the beam axis. The disks are glued on a transparent laser grade silica window (not shown in fig. 1) in order to position and hold the disk without perturbing the experiment. The light intensity distribution is recorded at a distance d, either on a screen and taking a picture with a camera or using a microscope in order to perform precise measurements, or using a CCD line camera (Thorlabs LC100) connected to a computer. All the experiment is set up on a non-vibrating table and the vortex phase plate and the lenses are settled on micrometre translation stages for precise alignment purposes. The alignment is performed directly looking at the diffracted dark spot on the screen, with the naked eye.

Theoretical considerations. – The diffraction of an usual infinite plane wave by a spherical opaque obstacle or by an opaque disk is a well-known calculation [2]. For the case of a LG beam with a topological charge l and for a spherical obstacle which centres are aligned, a standard analysis leads to an electric field E proportional to the l-order Bessel function J_l [20],

$$E(r,\theta) \approx J_l(\alpha r)\exp(il\theta), \tag{1}$$

where r and θ are the usual polar coordinates and

$$\alpha = 2\pi R/\lambda d, \tag{2}$$

where $2R$ is the diameter of the diffracting disk, λ is the laser wavelength and d is the distance between the obstacle and the observation zone. For the case $l=0$, the diffracted beam which is deduced from the J_0 Bessel function has a maximum on the axis of the beam and corresponds to the usual Arago-Poisson spot. However, for $l>0$, the J_l Bessel function and thus the diffracted beam has a null intensity on the axis. The position of the first maximum, deduced from the J_l Bessel function, is found to vary linearly with l.

We note in eq. (1) that the diffracted beam keeps its $\exp(il\theta)$ variation, still carrying the same angular momentum per photon as the initial LG beam. Since the calculations are valid for a wave carrying angular momentum and a spherical diffracting object, these results and consequences are not specific to the optical domain and should be also true for X-rays, microwaves, acoustics waves, seismic waves and for particles.

We also remark, according to eq. (2), that for a given topological charge l, the electric field profile should be exactly the same, whatever the wavelength, the distance between the diffracting object and the observation, or the size of the diffracting object. There is just a homothetic factor on the electric field or on the intensity profile. This means, in particular, that the size of the spot should vary linearly as a function of the distance d and of the wavelength λ and should be inversely proportional to the diameter of the diffracting opaque disk $2R$, as for the usual Arago-Poisson bright spot. The diffracted light intensity profile has been then readily calculated on a computer, using Matlab software, for several l orders of the LG beam.

Results. – Figure 2 shows pictures of the diffracted LG beam with a 7 mm diameter diffracting disk and at a distance of 3.5 m, together with the corresponding calculations, for several topological charges ($l=1$, $l=3$, $l=6$, $l=8$). Note that we have also seen diffracted LG beams for $l=2,4,5,7$ values but for clarity we have limited ourselves to four values. One clearly observes a dark spot appearing at the centre of the diffracted beam. This means that for non–zero-order LG beams, the Arago-Poisson bright spot is replaced by a tiny dark spot, as already noticed previously [20]. These observations could also be

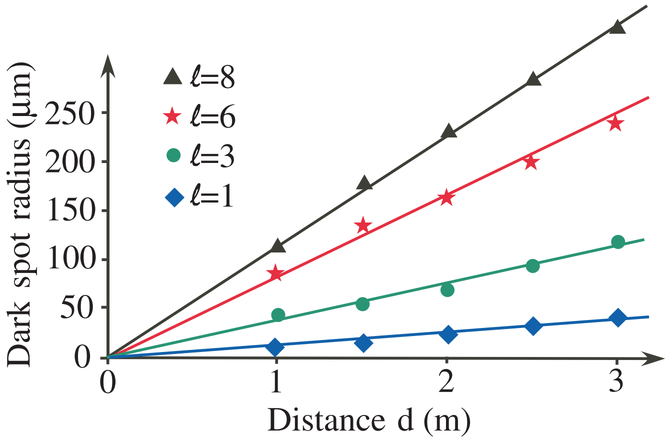

Fig. 3: (Colour on-line) Experimental variation of the size of radius R_d (HWHM) of the LG dark spot *vs.* d, the distance between the diffracting opaque disk and the detection zone, for various orders l of the LG beam and for a 7 mm diameter diffracting disk. Relative uncertainty: less than 3%. Solid straight line: guide for the eye according to eq. (2).

performed with the naked eye as well. Such diffraction figures of LG beams are well reproduced by the numerical simulations (see fig. 2) although the simulated dark zone is a little bigger (less than 5%) than with the experimental results. Typically, the LG dark zone is of the order of 50 μm for $l=1$ and 400 μm for $l=8$.

One also notices in fig. 2 that the size of the dark zone is increasing with the topological charge l of the LG beam. Besides, this dark spot really corresponds to a zero intensity zone. The edges of this spot are very well defined and get sharper as the topological charge l of the LG beam increases. Such a LG dark spot can be seen at a distance d varying from 1 m after the diffracting disk (LG dark-spot radius 7 μm for $l=1$), up to 10 m (LG dark-spot radius 70 μm for $l=1$). d is limited to 10 m due to our experimental apparatus. This means in particular that the diffracted LG beams by a disk also have the same surprising non-diffracting properties as the fundamental diffracted beam [23] while it propagates. This is absolutely not the case for an usual propagating Gaussian beam where a tightly focused Gaussian beam rapidly and strongly diverges except in a very small zone called the Rayleigh range [9]. Below a distance of 1 m, the diffracted laser intensity is too low to make any reliable quantitative measurement. The 7 μm dark-spot radius is the limit we can reach with a 7 mm diffracting disk and a 1 mW LG laser beam with $l=1$.

We have then plotted in fig. 3, the experimental size of the radius of the LG dark spot R_d *vs.* d, the distance between the diffracting opaque disk and the observation zone up to a distance of 3 m, for several topological charges l of the LG beam. The radius has been measured at Half-Width at Half-Maximum, HWHM. It is obtained either on the pictures of fig. 2 using ImageJ software to get the intensity profile, or on the intensity profile obtained with the CCD line camera. The figure exhibits a perfect linear variation of the size of the spot with the distance d between the diffracting object and the measurement plane, as expected from eq. (2). Indeed, according to eq. (2), the diameter size should vary as $\lambda d/R$. We have checked that this linear law still holds up to a distance of 10 m, *i.e.*, over one decade and for all the LG beam with topological charges varying from $l=1$ to $l=8$.

Moreover, one can also notice that the size of the LG dark zone increases with the topological charge l of the LG laser beam, as expected from eq. (1), since the width of the dip in the Bessel function representation increases with l. Actually, we have experimentally found a nearly linear variation with the topological charge l of the beam, in agreement with our calculations. We have checked that this law also holds for distances between the diffracting disk and the measurement zone up to $d=10\,$m.

Besides, we have changed the size of the diffracting opaque disk. At a distance of observation of $d=3$ m, we have measured the size of the radius R_d of the dark zone for three different opaque disks. For $l=8$, we found, with an uncertainty of at most $10\,\mu$m in this case: i) $R_d=310\,\mu$m for a diffracting disk diameter of $2R=7\,$mm, ii) $R_d=180\,\mu$m for a diffracting disk diameter of $2R=12\,$mm, and iii) $R_d=150\,\mu$m for a diffracting disk diameter of $2R=14$ mm. These values are in agreement with the expected values obtained with the theoretical calculations. The size of the LG dark spot decreases while increasing the size of the diffracting opaque disk. According to eq. (2), the diameter size should vary as $\lambda d/R$, *i.e.* such as the inverse of the diffracting opaque-disk radius. Actually, the above listed experimental values of the radius of the LG dark zone are in good agreement with this inverse law variation (see eq. (2)) and are in agreement with our calculations too. We have checked experimentally that the same variation also holds for the other l orders of the LG laser beam and for various distances d.

Finally, we have experimentally checked that these results are polarization independent, showing that, in our case, there is no coupling between the spin angular momentum and the angular orbital momentum [24]. The initial laser polarization is linear and is in the vertical direction. The rotation of the linear polarization by a half wave plate in front of the laser (horizontal polarization, oblique polarization) has no effect on the experimental diffraction figure. The use of a circular or elliptical polarization (rotation of a quarter wave plate in front of the laser) has no effect neither.

Discussion. – First of all, let us notice that this LG dark spot is completely different from the dark spot obtained in the absence of the diffracting disk. The dark spot is much smaller than with no diffracting mask. It keeps its shape along propagation while its size increases linearly. Moreover, this is totally different from what can be obtained with a telescope or upon focalization of a

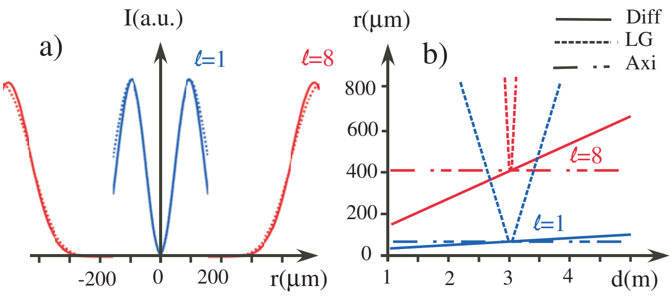

Fig. 4: (Colour on-line) a) Theoretical intensity profile of the $l = 1$ (blue) and $l = 8$ (red) diffracted LG laser beams (solid lines), LG focalized laser beams (dotted lines) that matches the diffracted LG beams at HWHM, and LG beams transformed by an axicon (dash-dotted lines) at a distance of 3 m. (b) Variation of the width of the vortex with the distance for the various beams. Note that the intensity profile of the diffracted beam at $d = 3$ m exactly matches the profile of the axicon generated beam at the same location, and is thus not visible in the figure.

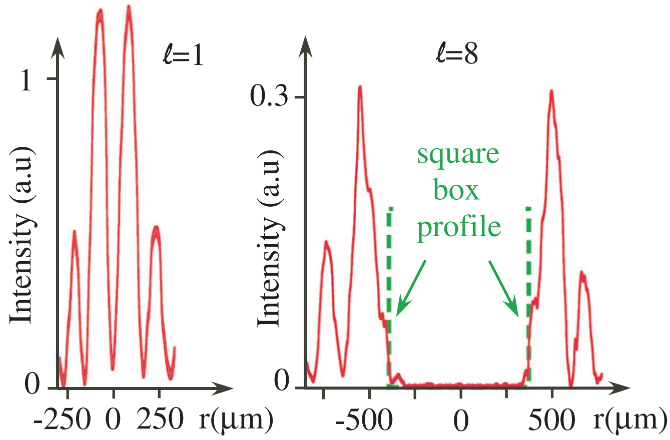

Fig. 5: (Colour on-line) Experimental intensity profiles of the $l = 1$ and $l = 8$ diffracted LG laser beams at a distance of 3 m recorded by the CCD line camera. Green dotted line: guide for the eye showing the ideal square box profile. Note the factor 3 between the intensity of the $l = 1$ and $l = 8$ diffracted beams.

LG beam (see fig. 4). We have plotted the theoretical intensity profiles of diffracted LG beams compared with the theoretical profile of vortex beams generated from focalized LG beams [9] and from LG beams followed by a conical surface lens called axicon (see fig. 4(a)). In fig. 4(b) we have plotted the variation of the width of the dark zone along propagation for these three beams. The intensity of the light scales as $r^{(2l)}$ for a focalized LG beam and it scales as $J_l^2(r)$ for a diffracted LG beam, as well as for the one generated with an axicon. For $l = 1$, the three intensity profiles nearly superpose, whereas, for $l = 8$, the intensity profile for the diffracted LG beam and for the axicon generated beam are slightly sharper (15% sharper) than for the focalized LG beam (see fig. 4(a)). Of course, the maximum intensity for the focalized LG beam is about twenty times higher than for the diffracted beam when optimized. However, and most of all, the focalized LG beam strongly diverges in the vicinity of the waist, whereas the diffracted LG beam and the axicon generated beam vary gently around this point (fig. 4(b)).

Besides, according to the linear variation of the dark-spot size of fig. 3 and according to the well-defined edges of the light intensity profile on the pictures of fig. 2, one may wonder what would be the ultimate possible size of the LG dark spot, for example, within the framework of atom guiding [25,26]. To that purpose, we have plotted in fig. 5, the intensity profiles obtained for $l = 1$ and $l = 8$ LG modes diffracted by a $2R = 7$ mm diameter disk. These profiles have been recorded by the CCD line camera and averaged ten times. The dip of the $l = 1$ LG beam is not very well pronounced. Actually, the shape of the profile must be parabolic. The resolution of our CCD camera introduces a convolution that affects the detected profile. Nevertheless, according to the theoretical profile of fig. 4(a) which have been confirmed by the microscope pictures, the profile of the $l = 1$ diffracted LG beam is far from a square profile. Conversely, for the $l = 8$ topological charge of the LG diffracted laser beam, we observe a very well-defined dark zone with no light in it and with rather sharp edges (nearly square box shaped). This is also confirmed by the theoretical profile of fig. 4(a). It simply means, as already noticed in [25] for Bessel beams, that the higher the topological charge of the LG diffracted beam, the better for the guiding of atoms.

Yet, a nearly one millimetre dark-zone diameter in the LG diffracted beam is really much too wide for the guiding of atoms. Nevertheless, since for a given l topological charge, all diffraction profiles are homothetic, one can increase the diffracting disk diameter $2R$ and reduce the distance between the diffracting disk and the observation zone d. This would lead to a smaller LG dark zone that exactly keeps the same shape. For example, with a 7 cm diameter disk, *i.e.*, ten times the diameter of the opaque disk that we used in fig. 5 and at a distance of 60 cm, *i.e.*, five times smaller than the distance d on the figure, the 500 μm scale would be replaced by a 10 μm scale. The radius of the dark zone of the $l = 8$ LG diffracted beam would then be 14 μm only, with very sharp and well-defined edges. The shape of the dark zone will still approach the ideal square box profile.

The use of the LG Arago-Poisson dark spot may thus be an alternative to the focusing of high topological charge LG beams which is not so obvious to perform [24] and needs LG beams with high-l purity, when a tiny dark zone in the centre of a bright light spot is needed. Since the Arago-Poisson dark spot is a non-diffracting beam, i) the same tiny dark zone holds for several meters of propagation, ii) the purity of the LG beam is not a determining factor any more: all the diffracted LG beams orders would have a small dark zone at the same position, all along propagation. The edges of the dark zone would be limited by the lower-order LG diffracted beam present in the initial beam. Besides, since the Arago-Poisson spot is only an interference effect [11,12], one can still use the paraxial approximation to calculate the propagation of such tiny LG dark-spot beams. Naturally, such beams would also have a supra-luminal propagation behaviour.

Of course, Bessel beams could be obtained by other means, for example by the use of a conical surface lens called axicon [25]. However, such axicon must be of high laser quality grade and must be perfectly aligned with the LG laser beam with very little aberrations. We did try to perform such experiments using axicons. We did not find experimentally intensity profiles better than the one shown in fig. 2. Actually, the axicon was very difficult to align properly. The central dark spot was hardly noticeable. It seemed that experimentally, there was always a tiny bright spot in the middle of the dark spot. Besides, the use of a simple disk is much easier and offers a better versatility than the use of an axicon. Only the diffracting disk has to be changed to modify the diameter of the LG dark zone at a given distance. However, with an axicon, the diameter of the dark spot is always rigorously the same along propagation (see fig. 4(a)) and the propagation distance is limited by the size and the aperture of the axicon. A small-size dark spot would lead to a small propagation distance. With the Arago-Poisson LG dark spot, the dark-spot zone is like a funnel and is not limited by the size of the opaque diffracting beam but is rather limited by the available intensity. Indeed, a lot of light power is useless or blocked by the diffracting disk. Only the diffracted light by the edges of the disk plays a role. Although the theoretical intensity profiles are exactly the same, such Arago-Poisson LG dark spots would require rather high-power lasers compared with dark-spot Bessel laser beams generated with axicons. Conversely, Arago-Poisson LG dark spots are easy to handle and to align experimentally.

Conversely, the $l=1$ LG diffracted beam could be of useful help in alignment procedures or accurate position measurements [10]. Indeed, the detection of a minimum intensity in an intensity profile is much easier to perform than the detection of a maximum intensity. There are no saturation effects on the detector, and the sensitivity of the detection can be increased. According to fig. 3 and fig. 5, a 10 μm (HWHM) LG dark-spot radius can be readily obtained with a 10 mm diffracting disk at a distance of the order of one meter. With the help of a position-sensitive diode mounted on a piezo stage, sub-micron precision alignment limits seem easily within reach.

Conclusion. – We have experimentally observed a dark spot (Arago-Poisson dark spot) in the shadow of a diffracting disk illuminated by a non-zero topological charge LG laser beam. The size of the spot depends on the topological charge l of the LG beam, on the distance between the diffracting disk and the measurement zone and on the diameter of the disk. LG dark spot having a few tens micrometer sizes, with l varying from 1 to 8, have been experimentally observed, in agreement with theory. This technique could be an alternative to the focalisation of high-order LG beams in the field of atoms guiding. Since one can obtain, in principle, micrometer size spots, it may also be used to perform spectroscopic measurements on atoms using beams carrying orbital angular momentum [27,28]. Besides, such diffraction phenomena should also exist in plasma vortex [29] and in astrophysics as well [30]. The Arago-Poisson LG dark spot could be an elegant way to detect the electromagnetic field, or even the gravitational field, that carries non-zero orbital angular momenta and which is emitted by a rotating black hole in the shadow of a planet, or a star, or a galaxy, or simply emitted by the Sun during a solar eclipse for example.

* * *

We acknowledge valuable help from J. R. Thébault and useful discussions with A. Bennis and A. Le Floch. This work was supported by the University of Rennes 1 via a "défi émergent" action. RN acknowledges financial support from the Région Bretagne and from the Direction Générale de l'Armement (DGA).

REFERENCES

[1] Sommerfeld A., *Optics* (Academic Press, New York) 1954.

[2] Born M. and Wolf E., *Principle of Optics*, 7th edition (Cambridge University Press, Cambridge) 1999.

[3] Hecht E., *Optics*, 4th edition (Addison-Wesley, San Fransisco) 2001.

[4] Fresnel A., *Œuvres complètes d'Augustin Fresnel*, Vol. **1** (Imprimerie Impériale, Paris) 1866, pp. 229–246, 365–372.

[5] Harvey J. E. and Forgham J. L., *Am. J. Phys.*, **52** (1984) 243.

[6] Evans P., Rogers K., Chan J., Rogers J. and Dicken A., *Appl. Phys. Lett.*, **97** (2010) 204101.

[7] Macaulay E. J., Hartmanna W. M. and Rakerd B., *J. Acoust. Soc. Am.*, **127** (2010) 1440.

[8] Reisinger T., Patel A. A., Reingruber H., Fladischer K., Ernst W. E., Bracco G., Smith H. I. and Holst B., *Phys. Rev. A*, **79** (2009) 053823.

[9] Siegman A. E., *Lasers* (University Science Books, Mill Valley) 1990.

[10] Saruta K. and Tsuji R., *Jpn. J. Appl. Phys.*, **46** (2007) 6000.

[11] Chauvat D., Emile O., Brunel M. and Le Floch A., *Phys. Lett. A*, **295** (2002) 78.

[12] Chauvat D., Emile O., Brunel M. and Le Floch A., *Am. J. Phys.*, **71** (2003) 1196.

[13] Allen L., Beijersbergen M. W., Spreeuw R. J. C. and Woerdman J. P., *Phys. Rev. A*, **45** (1992) 8185.

[14] van Enk S. J. and Nienhuis G., *Europhys. Lett.*, **25** (1994) 497.

[15] Allen L., Barnett S. M. and Padgett M. (Editors), *Optical Angular Momentum* (IOP, Bristol) 2003.
[16] Thidé B., Then H., Sjöholm J., Palmer K., Bergman J., Carrozzi T. D., Istomin Y. N., Ibragimov N. H. and Khanitova R., *Phys. Rev. Lett.*, **99** (2007) 087701.
[17] Silva G. T., Lobo T. P. and Mitri F. G., *EPL*, **97** (2012) 54003.
[18] McMorran B. J., Agrawal A., Anderson I. M., Herzing A. A., Lezec H. J., McClelland J. J. and Unguris J., *Science*, **331** (2011) 192.
[19] Hickmanna J. M., Fonseca E. J. S. and Jesus-Silva A. J., *EPL*, **96** (2011) 64006.
[20] Fischer P., Skelton S. E., Leburn C. G., Streuber C. T., Wright E. M. and Dholakia K., *Opt. Express*, **15** (2007) 11860.
[21] Beijersbergen M. W., Coerwinkel R. P. C., Kristensen M. and Woerdman J. P., *Opt. Commun.*, **112** (1994) 321.
[22] Mari E., Tamburini F., Swartzlander G. A., Bianchini A., Barbieri C., Romanato F. and Thidé B., *Opt. Express*, **20** (2012) 2445.
[23] Durnin J., Miceli J. J. and Eberly J. H., *Phys. Rev. Lett.*, **58** (1987) 1499.
[24] Klimov V. V., Bloch D., Ducloy M. and Leite J. R. R., *Phys. Rev. A*, **85** (2012) 053834.
[25] Arlt J., Hitomi T. and Dholakia K., *Appl. Phys. B*, **71** (2000) 549.
[26] Mestre M., Diry F., Viaris de Lesegno B. and Pruvost L., *Eur. Phys. J. D*, **57** (2010) 87.
[27] Barreiro S. and Tabosa J. W. R., *Phys. Rev. Lett.*, **90** (2003) 133001.
[28] Han L., Cao M., Liu R., Guo W., Wei D., Gao S., Zhang P., Gao H. and Li F., *EPL*, **99** (2012) 34003.
[29] Tamburini F., Sponselli A., Thidé B. and Mendonça J. T., *EPL*, **90** (2010) 45001.
[30] Tamburini F., Thidé B., Molina-Terriza G. and Anzolin G., *Nat. Phys.*, **7** (2011) 195.